

On function homophily of microbial Protein-Protein Interaction Networks

Nicola Apollonio^a, Paolo Giulio Franciosa^b, Daniele Santoni^{c,*}

^a*Istituto per le Applicazioni del Calcolo “Mauro Picone”, Consiglio Nazionale delle Ricerche, Via dei Taurini 19, 00185 - Rome, Italy*

^b*Dipartimento di Scienze Statistiche, Sapienza Università di Roma, P.le Aldo Moro 5, 00185 - Rome, Italy*

^c*Istituto di Analisi dei Sistemi ed Informatica “Antonio Ruberti”, Consiglio Nazionale delle Ricerche, Via dei Taurini 19, 00185 - Rome, Italy*

Abstract

We present a new method for assessing homophily in networks whose vertices have categorical attributes, namely when the vertices of networks come partitioned into classes. We apply this method to Protein-Protein Interaction networks, where vertices correspond to proteins, partitioned according to their functional role, and edges represent potential interactions between proteins.

Similarly to other classical and well consolidated approaches, our method compares the relative edge density of the subgraphs induced by each class with the corresponding expected relative edge density under a null model. The novelty of our approach consists in prescribing an endogenous null model, namely, the sample space of the null model is built on the input network itself. This allows us to give exact explicit expression for the **z**-score of the relative edge density of each class as well as other related statistics. The **z**-scores directly quantify the statistical significance of the observed homophily via Čebyšev inequality. The expression of each **z**-score is entered by the network structure through basic combinatorial invariant such as the number of subgraphs with two spanning edges. Each **z**-score is computed in $O(n^3)$ worst-case time for a network with n vertices. This leads to an overall effective computational method for assessing homophily. Theoretical results are then exploited to prove that Protein-Protein Interaction networks networks are significantly homophilous.

Keywords: Protein-Protein Interaction Networks, Protein function, Homophily

1. Introduction

Proteins are biological macromolecules made of amino acid chains. According to the major paradigm in molecular biology, known as *Central Dogma*, genetic information flows from DNA to RNA and finally to proteins, that constitute the engine of living organism cells performing a large variety of functions. Proteins are at the basis of every functional task inside and outside the cell but the huge complexity, characterizing living organisms, is mostly due to their ability to interact each other. The complexity of such interactions is trivially quadratic with the number of proteins and can be modeled as a graph, made of a set of protein vertices and a set of edges representing potential interactions between proteins. Those graphs, known as Protein-Protein Interaction (PPI) networks, are ideally able to capture every relationship among proteins and are often used to shed light on the whole system biology of cells. There exist different kind of PPIs, depending on the way they estimate interactions in terms of computational models and considered data sources.

PPI networks can be derived from literature, through text mining of scientific texts, or can be computationally predicted through genomic features analysis, or inferred from model organisms based on orthology. Bayesian methods are often used to combine probability scores coming from different data sources [6, 1]. Proteins can be naturally associated with functional classes, depending on the role they play in the cell and this classification yields a *functional description* of PPI networks, where membership of a vertex (protein) to its own functional class can be seen as a categorical attribute of the vertex (also

*Corresponding author.

Ph.: +39 06 49937119. Fax: +39 06 .49937137
email address: daniele.santoni@iasi.cnr.it

referred to a color). The basic way to model interactions in networks is simply by the adjacency relation among their vertices, namely, two vertices of a (PPI) network interact when they are connected by an edge. In this respect the topology of a given network is thought of as its *geometrical description*.

It is biologically relevant to study whether the functional description correlates with the geometrical description of PPI networks or, equivalently, whether the attributes of vertices correlate across edges. Networks exhibiting a high such correlation are known as *homophilous* or *assortative mixing*. In general, a network might be homophilous (or mix assortativity) with respect to given attributes, while it might be heterophilous (or *disassortative*) with respect to others—for instance, PPI networks are disassortative with respect to vertex degree [7].

Often, social networks exhibit homophily with respect to attributes such as gender, age, ethnicity, occupation, social class and many others. This simply means that vertices preferentially interact with vertices sharing the same attribute value. On the opposite, heterophilous networks are those networks whose vertices preferentially interact with vertices having different attributes values. Putting it succinctly: “birds of a feather flock together” [3].

Homophily in networks certainly fits in the frame of “community detection” (communities in complex networks identify high order homogeneous structures) [9, 5]. Arguing as in [20], network community detection can be seen as a procedure consisting of two stages: one stage consists of extracting communities by relying on the geometric structure of the networks, while the second stage consists in “abstracting” communities, namely, in identifying the common features and attributes of community members (functional class proteins in our case). From this perspective, communities are first detected based on their geometry and then evaluated based on their functions. In our case we take the other way round: we are given a functional description of the communities and we try to assess whether or not such communities have a certain amount of geometrical structure.

In this framework, network homophily and communities are strictly connected with the paradigm of *Guilt by Association* (GAS) [11]. According to this paradigm, the function of a given protein can be inferred by analyzing the function of its neighbours [2, 13]. It was anyway highlighted how GAS requires a deep analysis, since information coming from neighbours has to be evaluated selecting those critical interactions that could have a major role in determining protein role [4].

In this paper, we study homophily in PPI networks with respect to their functional description, namely when the attribute value of a vertex is simply the functional class it belongs to. We propose a new statistical model that builds on the approach in [12] (developed for networks with only two functional classes), extends it to an arbitrary number of classes, and strengthens it by exploiting second order statistics based on certain random colorings of the input network. This machinery yields an explicit exact formula for the **z**-score of a suitable defined homophily index as well as of the number of isolated vertices of each functional class. The statistical significance of the observed homophily is then obtained through Čebyšëv inequality. As one may expect, the structure of the network enters second order statistics through the number of its subgraphs with two spanning edges, namely, the number of its P_3 ’s (if the two edges are adjacent) and the number of its $2K_2$ ’s (if the two edges are not adjacent)¹. This means that our analysis does not require exogenous models (random graphs, for instance) to make comparisons for assessing homophily. Our theoretical results are then applied to ten PPI networks, mainly derived from Bacteria (8 organisms belonging to different Phyla or classes). Moreover, *Saccharomices cerevisiae* (Fungi - Ascomycota) and *Pyrococcus abyssi* (Euryarcheota - Thermococci) were included in the study for comparison.

2. Materials and Methods

Protein-Protein Interaction networks. In this study we consider ten organisms. The related PPI networks were retrieved from STRING database (<https://string-db.org/>) [16, 17], setting a high confidence cutoff (700, corresponding to a 0.7 likelihood). The selected organisms are mainly Bacteria (8 out of 10 belonging to different Phyla or classes), we also included in the study *Saccharomices cerevisiae* (Fungi - Ascomycota) and *Pyrococcus abyssi* (Euryarcheota - Thermococci) for comparison. The 8 bacterial organisms were chosen as representatives of Bacteria Kingdom, including different Phyla (Alpha, Gamma,

¹ P_3 is the graph on three vertices joined by two edges, while $2K_2$ is the graph on four vertices and with two edges without common endpoints.

Epsilon protobacteria, Actinobacteria, Firmicutes/Bacilli, Spirochaetes). Organisms were also chosen on the basis of their network sizes (number of vertices and edges), in order to build an etherogeneous dataset. Species, Kingdom, Phylum/Class as well as number of vertices and edges in the relative network are reported in Tab. 1 for each organism.

Organism			PPI	
Species	Kingdom	Phylum/Class	vertices	edges
Brucella Melitensis (Bm)	Bacteria	Alphaproteobacteria	2,675	15,450
Escherichia coli (Ec)	Bacteria	Gammaproteobacteria	4,020	29,748
Haemophilus influenzae (Hi)	Bacteria	Gammaproteobacteria	1,609	9,202
Helicobacter pylory J99 (Hp)	Bacteria	Epsilonproteobacteria	1,264	7,678
Mycobacterium tuberculosis H37Rv (Mt)	Bacteria	Actinobacteria	3,779	24,889
Streptococcus pneumoniae TIGR4 (Sp)	Bacteria	Firmicutes/Bacilli	1,811	8,813
Treponema pallidum (Tp)	Bacteria	Spirochaetes	8,94	8,157
Vibrio cholerae (Vc)	Bacteria	Gammaproteobacteria	3,153	20,844
Pyrococcus abyssi (Pa)	Euryarchaeota	Thermococci	1,564	9,090
Saccharomyces cerevisiae (Sc)	Fungi	Ascomycota/Saccharomycetes	6,157	119,051

Table 1: organisms

Functional protein classes. Functional classes of proteins of the considered ten organisms were obtained from NCBI database (<ftp://ftp.ncbi.nih.gov/pub/COG/COG/>). Proteins were partitioned in 25 different functional classes, but only 19 were taken into account in this work, since:

- 5 classes (A - RNA processing and modification, B - Chromatin structure and dynamics, Y - Nuclear structure, Z - Cytoskeleton, W - Extracellular structures) had no representatives (or only a few) for most of bacterial organisms;
- classes R - general function prediction, and S - Function unknown, were merged into the X class.

The 19 considered classes are reported in Tab 2.

INFORMATION STORAGE AND PROCESSING	
J	Translation, ribosomal structure and biogenesis
K	Transcription
L	Replication, recombination and repair
CELLULAR PROCESSES AND SIGNALING	
D	Cell cycle control, cell division, chromosome partitioning
V	Defense mechanisms
T	Signal transduction mechanisms
M	Cell wall/membrane/envelope biogenesis
N	Cell motility
U	Intracellular trafficking, secretion, and vesicular transport
O	Posttranslational modification, protein turnover, chaperones
METABOLISM	
C	Energy production and conversion
G	Carbohydrate transport and metabolism
E	Amino acid transport and metabolism
F	Nucleotide transport and metabolism
H	Coenzyme transport and metabolism
I	Lipid transport and metabolism
P	Inorganic ion transport and metabolism
Q	Secondary metabolites biosynthesis, transport and catabolism
POORLY CHARACTERIZED	
X	Function unknown or general function prediction only

Table 2: Functional Classes

Parsing networks and building data structures. Each organism’s network is an undirected graph, in which each vertex represents a protein associated to a color denoting one of the functional classes listed in Table 2, and each edge represents the interaction between two proteins, weighted according to the likelihood of the given interaction.

A PPI graph is thus represented by two text files, the first lists vertex labels and the associated colors, the second lists edges as pairs of vertices and the associated weight in range [0, 999]. Edges have been cut-off at a 700 minimum weight, usually considered as a high confidence threshold. Isolated vertices in the resulting graph have been deleted. Some networks present a very limited number of vertices (some units) labeled by similar values (e.g., `jhp0681_1` and `jhp0681_2` in the vertex file for organism *Helicobacter pylori*) representing different isoforms of the same protein, but these vertices were simply denoted by a unique label (e.g., `jhp0681`) in the edge listing file. We merged such vertices in a single vertex; in the few cases in which they were associated to different functional classes, we merged them associating the functional class X to that vertex.

Our experiments have been conducted on an Intel Core i5 machine with 4 cores, 2.3 GHz clock, 16 GB RAM, 256 KB L2 cache and 6 MB L3 cache, equipped with MAC OS 10.14.6.

All methods have been written in Python 3 and executed by a Python 3.7.2 interpreter, exploiting package *NetworkX*, version 2.5.

3. Homophily in networks

As said in Section 1, homophily is a network property occurring when the attributes of the vertices correlate across the edges. When attributes of vertices are the labels (colors) of the functional classes they belong to in some functional description, this means essentially that the subgraphs induced by the vertices of the same color are relatively denser than what we expect under some suitable null model (the relative edge density of a subgraph of a given graph G is the fraction of the edges of the subgraphs over the total number of edges in the graph). Newman’s celebrated *modularity* index [10] formulates the

null hypothesis as the relative expected density of a random graph with the same degree distribution as the input graph. Modularity is thus the relative edge density of monochromatic subgraphs minus the expected relative edge density of monochromatic subgraphs under the null hypothesis that edges are distributed at random among vertices. Since the index lies in interval $[-\frac{1}{2}, 1]$, its value directly quantifies network homophily: the larger the index the more homophilous the network is. Modularity thus provides a scale for comparing homophily of different networks. Notice that Newman's index resorts to an exogenous model (the *configuration model*) to test homophily. In this paper, by revising the idea in [12], we propose to measure network homophily by testing the observed structure (i.e., the relative edge density of functional classes) against the expected structure under an endogeneous random model: the input graph itself will be the sample space for the null hypothesis. In this way we can answer the question "how homophilous the network is" without comparing it with other networks (see discussion at the end of Section 3.3). Let us now discuss the approach in [12] in more detail.

3.1. Existing models

The simple original definition of homophily in [12] refers to the case of two non overlapping classes, thus defined by a function assuming only two values, let's say 0, 1, on the vertices of a given simple undirected graph G with n vertices and m edges. Such values are thought of as properties the vertices of G can have. Edges of G are then classified as (0, 0)-edges, (0, 1)-edges and (1, 1)-edges according to the property at their endvertices. Let c_0 (resp., c_1) be the number of vertices of G having property 0 (resp., 1), with $c_0 + c_1 = n$; furthermore, let $m_{i,j}$ be the number of (i, j) -edges, $i, j \in \{0, 1\}$, with $m_{0,0} + m_{0,1} + m_{1,1} = m$: if the functional definition of the communities correlated with the structure of G , then we should expect a statistical significant deviation between $m_{0,0}$, say, and what we would expect if property 0 were randomly distributed among the vertices of the graph, namely, if any vertex had an equal chance of possessing it. In [12], it is proposed to measure this deviation by the three ratios:

$$\omega_0 = \frac{m_{0,0}}{\overline{m}_{0,0}}, \quad \eta_{0,1} = \frac{m_{0,1}}{\overline{m}_{0,1}}, \quad \omega_1 = \frac{m_{1,1}}{\overline{m}_{1,1}}$$

where, for $i, j \in \{0, 1\}$ and $i \neq j$

$$\overline{m}_{i,i} = m \frac{c_i(c_i - 1)}{n(n - 1)} \quad \text{and} \quad \overline{m}_{i,j} = m \frac{2c_i c_j}{n(n - 1)},$$

are the expected number of (i, i) -edges and (i, j) -edges, respectively, under the hypothesis that properties 0 and 1 are randomly distributed over the vertex set of G (see Section 3.3 for proofs). Just by rewriting ω_i and $\eta_{i,j}$ as

$$\omega_i = \frac{2m_{i,i}}{c_i(c_i - 1)} \Big/ \frac{2m}{n(n - 1)} \quad \text{and} \quad \eta_{i,j} = \frac{m_{i,j}}{c_i c_j} \Big/ \frac{2m}{n(n - 1)} \quad (1)$$

one sees that ω_i is nothing but the normalized intracommunity density; analogously, $\eta_{i,j}$ is the normalized intercommunity density [20]. In this perspective, homophily (and heterophily) provides a suggestive interpretation of basic structural graph properties (those that can be captured by first order moments of functions of random partitions into two classes with c_0 vertices labeled 0 and c_1 vertices labeled 1). In this simple model, graph G is declared i -homophilous (or homophilous with respect to property i), $i \in \{0, 1\}$, if $\frac{m_{i,i}}{\overline{m}_{i,i}} > 1$; graph G is declared (i, j) -heterophilous if $\frac{m_{i,j}}{\overline{m}_{i,j}} > 1$ (we ask the reader to bear the pedantic reference to the indices i, j in view of the generalization to more than 2 properties). Without any other clue about the likelihood or the variability of ω_i and $\eta_{i,j}$, it is clear that both the assertions have no statistical significance behind their descriptive power. Moreover, it follows from (1) that ω_i lies in the interval $[0, 1/\rho(G)]$, $\rho(G)$ being the edge density of G and such an interval might be really wide for sparse graphs. To overcome this limitation, [12] developed a computational model (feasible only for the case of two colors) aimed at evaluating the likelihood of an observed instance $(\omega_0, \eta_{0,1})$ in the form of a phase diagram in the $m_{0,0}m_{0,1}$ -plane. Each point of such a diagram is the frequency of all partitions of the vertex set G into two parts C_0 and C_1 with c_0 and c_1 vertices, respectively, such that the subgraph of G induced by C_0 has $m_{0,0}$ edges, while the subgraph induced by C_1 has $m - (m_{0,0} + m_{0,1})$ edges, m being the size of G . The diagram is computed by exhaustive enumeration for small graphs, while for large graphs only the boundary of the diagram is heuristically computed. In either cases, the likelihood of the observed pair is determined by its position and its darkness (in a grayscale) in the phase diagram.

Although this approach has been proven successfully for a wide range of real networks (with only two functional classes), including certain PPI networks [12], it still suffers of the following limitations:

- (a) it is computationally expensive;
- (b) it is applicable only to two functional classes;
- (c) it is rather qualitative.

To remedy these limitations, we propose to compute the **z-score** of ω_i and $\eta_{i,j}$ under the null model described in the next section. Since, as we show, this can be done for any number of colors in $O(n^3)$ worst-case time, (a) and (b) are settled. As for (c), if Z_i , say, is the **z-score** of ω_i , then by Čebyšev inequality the probability of the event $(Z_i > \lambda)$ is at most λ^{-2} under the null model. Hence Z_i^{-2} directly measures the statistical significance of ω_i , at the same time making the method completely quantitative.

3.2. Design of the new model

As we said, Protein-Protein Interaction Networks are graphs whose vertices are proteins and whose edges model potential interactions between proteins. Since proteins are classified by the biological function they are responsible for, each protein is uniquely associated with one of the 19 function classes listed in Table 2 and which we identify by their labels. Therefore, given a PPI network G , the correspondence protein \rightarrow function defines a surjective map g from the set of vertices of G into a set of 19 labels and, after thinking of the labels as colors, such a correspondence will be referred to as a *coloring*. The input of our model is thus a pair (G, g) consisting of an undirected graph G (the given PPI network) and a coloring $g : V(G) \rightarrow [s]$, where s is a positive integer fixed once and for all (in our case $s = 19$) and, as customary, we have set $[s] = \{1, \dots, s\}$ for shortness. Hence, G encodes the geometrical description of the network and g encodes its functional description. The *i-th functional class* is the set $g^{-1}(i)$ consisting of the vertices of G having color i , namely, functional classes are identified with color classes under g . These classes are our communities. Let c_i , $i \in [s]$, be the number of vertices of G of color i and call the integer vector $\mathbf{c} = (c_1, \dots, c_s)$ the *profile* of g . Any surjective map $f : V(G) \rightarrow [s]$ with the same profile as g will be referred to as a *c-coloring* of $V(G)$ (or simply *c-coloring* when $V(G)$ is understood). Our next step is to introduce a probability space that allows us to formulate null hypotheses to test against alternative hypotheses about (G, g) . To this end, let $\Phi(\mathbf{c})$ be the set of all *c-colorings* of $V(G)$. Since the *multinomial coefficient* with parts $c_1, c_2 \dots c_s$, denoted by one of the two symbols below

$$\binom{n}{\mathbf{c}}, \quad \binom{n}{c_1 c_2 \dots c_s},$$

counts the *c-colorings* of $V(G)$ (see Section 6), it follows that $|\Phi(\mathbf{c})| = \binom{n}{\mathbf{c}}$. A *random c-coloring* is the random variable F with values in $\Phi(\mathbf{c})$ and with probability mass function given by

$$\mathbb{P}_{n,\mathbf{c}}(F) = \Pr\{F = f\} = \binom{n}{\mathbf{c}}^{-1},$$

namely, all *c-colorings* are equally likely (see Section 6 for a more formal definition not needed here). Having the probability space $(\Phi(\mathbf{c}), \mathbb{P}_{n,\mathbf{c}})$ we test functions of (G, g) versus the same functions under the null hypothesis (G, F) , where F is a random *c-coloring* of $V(G)$. We therefore define several random variables as functions of the random variable F , and such variables enable us to give first and second order moments of those statistics crucial for our purposes. We close this section by describing the former ones, deferring the description of the latter ones to the next section.

For a vertex $v \in V(G)$ and a color $i \in [s]$, let X_v^i be the Bernoulli random variable that equals to 1 if and only if vertex v has color i under the random *c-coloring* F , i.e., X_v^i is the indicator of the event $F(v) = i$. Since X_v^i is a Bernoulli random variable, by (13) (refer to Section 6), one has

$$\mathbb{E}(X_v^i) = \Pr\{X_v^i = 1\} = \frac{c_i}{n}.$$

Analogously, for the product of two such variables for $u, v \in V$, $u \neq v$, and $i, j \in [s]$, after resorting to (13) and (14) (Section 6) one has

$$\mathbb{E}(X_u^i X_v^j) = \Pr\{X_u^i X_v^j = 1\} = \Pr\{X_u^i = 1, X_v^j = 1\} = \begin{cases} \frac{c_i^2}{n^2} & \text{if } i = j \\ \frac{c_i c_j}{n^2} & \text{if } i \neq j. \end{cases} \quad (2)$$

where, after adhering to the notation in [8], for a positive integer a and a nonnegative integer r , we have denoted by the symbol $a^{\underline{r}}$ the *falling r -th power* of a (see also Section 6 for more details), namely $a^{\underline{r}} = a(a-1) \cdots (a-r+1)$, with $a^{\underline{0}} = 1$. Thus, the 2-nd falling power $a^{\underline{2}}$ of a equals $a(a-1)$. The above formula immediately shows that the random variables X_v^i as v runs in $V(G)$ and i runs in $[s]$ are not independent (neither are X_u^i and X_v^j). Without pretending to be rigorous, this is only due to the fact that a random \mathbf{c} -coloring can be thought of as the outcome of experiments where one draws from a bin “without replacement”. However, variables in $\{X_v^j \mid v \in V, j \in [s]\}$ are *exchangeable*, in the sense that the joint distribution of any subset of them does not depend on the order of drawing (the distribution is symmetric with respect to permuting indices). Hence, as long as we consider statistics based only on linear combinations of X_v^i , there is no other dependency other than the one inherited by the sampling procedure. To let the graph come into the structure of the dependency among variables, we have to consider second order statistics.

Let us come to edges now and, for an edge $uv \in E(G)$ and colors $i, j \in [s]$, let $Y_{uv}^{i,j}$ be the Bernoulli random variable which is equal to 1 if and only if one of the endvertices of uv has color i and the other one has color j . Hence, if $i = j$, then $Y_{uv}^{i,i} = X_u^i X_v^i$ while if $i \neq j$, then $Y_{uv}^{i,j} = X_u^i X_v^j + X_u^j X_v^i$. Therefore by (2)

$$\mathbb{E}(Y_{uv}^{i,j}) = \Pr\{Y_{uv}^{i,j} = 1\} = \begin{cases} \frac{c_i^2}{n^2} & \text{if } i = j \\ 2\frac{c_i c_j}{n^2} & \text{if } i \neq j. \end{cases} \quad (3)$$

One more random variable is needed to compute the first two moments of the statistics we are interested in. Let T be a nonempty subset of $V(G)$ and let $i \in [s]$ be a color; define D_T^i as the number of elements of T having color i ; by definition, D_T^i has the following expression:

$$D_T^i = \sum_{v \in T} X_v^i$$

Let A and B be disjoint subsets of $V(G)$. To determine the distribution of D_T^i we are interested in the probability of the event that all the elements of A have color i while all those of B have not. Let $\Omega_i(A, B)$ denote this event (for more on events on this type refer to Section 6). Thus

$$\Omega_i(A, B) = (F(a) = i, \forall a \in A) \wedge (F(b) \neq i, \forall b \in B).$$

Hence

$$(D_T^i = h) = \bigvee_{\substack{R \subseteq T \\ |R|=h}} \Omega_i(R, T \setminus R)$$

and since the events on the right hand side of the identity above are mutually incompatible, after (11) and after setting $t = |T|$, one has

$$\Pr\{D_T^i = h\} = \binom{t}{h} \frac{\frac{h}{n}(n - c_i)^{t-h}}{n^t} \quad (4)$$

and the close resemblance with the binomial distribution with parameters t and $\frac{c_i}{n}$ is clear: powers are replaced by falling powers. This is not an accident: D_T^i follows a hypergeometric distribution $\text{Hyp}(n, c_i, t)$ giving the probability of success by drawing without replacement t balls from an urn containing n balls, c_i of which are successfull. By choosing T equal to the neighborhood of a vertex $v \in V(G)$, one immediately gets the distribution of the random number of neighbors of vertex v with color i , i.e., $D_{N_G(v)}^i \sim \text{Hyp}(n, c_i, \deg_G(v))$.

3.3. Homophily, heterophily and isolated vertices: first and second order moments

We are now in position to describe statistics capable of assessing whether PPI networks are homophilous. Let (G, g) be a pair consisting of a PPI network G with n vertices and m edges and a \mathbf{c} -coloring g . As we did in Section 3.1, we classify the m edges of G according to the colors of their endvertices. Consequently, we say that edge $uv \in E(G)$ is a (i, j) -edge of (G, g) if $\{g(u), g(v)\} = \{i, j\}$, $i, j \in [s]$ —with a little abuse of notation we also admit $i = j$. Notice that (i, i) -edges are the edges of G induced by the vertices in color class i (those responsible for the homophily of (G, g)) and, for $i \neq j$,

(i, j) -edges are the edges with one endvertex in color class i and the other one in color class j (those responsible for the heterophily of (G, g)). Let $m_{i,i}$ and $m_{i,j}$ be the number of (i, i) -edges and (i, j) -edges of (G, g) , respectively. Therefore, for any two (possibly equal) colors $i, j \in [s]$, the random variable

$$M^{i,j} = \sum_{uv \in E(G)} Y_{uv}^{i,j}$$

counts the number of (i, j) -edges of (G, F) where F is a random \mathbf{c} -coloring. Let $\bar{m}_{i,j}$ be the expected value of $M^{i,j}$: by (3) and the linearity of expectation it follows straightforwardly that

$$\bar{m}_{i,j} = \begin{cases} m \frac{c_j^2}{n^2} & \text{if } i = j \\ 2m \frac{c_i c_j}{n^2} & \text{if } i \neq j. \end{cases}.$$

which generalizes to an arbitrary number of colors the corresponding expressions given in Section 3.1 for two colors. Analogously, we define the i -homophily of (G, g) and (i, j) -heterophily of (G, g) , $i \neq j$, as the ratios

$$\omega_i = \frac{m_{i,i}}{\bar{m}_{i,i}}, \quad \eta_{i,j} = \frac{m_{i,j}}{\bar{m}_{i,j}}.$$

If for all $i, j \in [s]$ (possibly $i = j$) we knew the variance $\sigma_{i,j}^2$ of $M^{i,j}$, then we could compute the **z-score** of the observed ω_i e $\eta_{i,j}$ as the ratios

$$Z(\omega_i) = \frac{m_{i,i} - \bar{m}_{i,i}}{\sigma_{i,i}} = Z(m_{i,i}), \quad Z(\eta_{i,j}) = \frac{m_{i,j} - \bar{m}_{i,j}}{\sigma_{i,j}} = Z(m_{i,j}). \quad (5)$$

By Čebyšev inequality, if we assume, for instance, the null hypothesis that the observed value ω_i is a value assumed by the random variable $\frac{M^{i,i}}{\bar{m}_{i,i}}$ in the probability space $(\Phi(\mathbf{c}), \mathbb{P}_{\mathbf{c},n})$ —which is tantamount to assume that (G, g) does not display i -homophily—then the confidence level for accepting the null hypothesis would be at most $Z^{-2}(\omega_i)$. Deferring for a while the computation of $\sigma_{i,j}^2$, let us examine another useful statistic for (G, g) : the number l_i of isolated vertices of color i , i.e., the number of vertices in color class i having no neighbors in color class i . Call any such vertex i -isolated and observe that by definition the number of i -isolated vertices is

$$l_i = |\{v \in V(G) \mid g(v) = 1 \wedge g(w) \neq i, \forall w \in N_G(v)\}|.$$

Let L^i be the random variable defined as the number of i -isolated vertices of (G, F) where F is a random \mathbf{c} -coloring of $V(G)$. Although the random variables L^i 's and $M^{i,i}$'s are clearly dependent—at the extreme cases, for instance, $\Pr\{M^{i,i} = 0 \mid L^i \geq c_i - 1\} = 1$ and $\Pr\{M^{i,i} \geq \frac{c_2}{2} \mid L^i = 0\} = 1$ —the joint knowledge of corresponding statistics l_i and ω_i is still quite informative. Indeed, consider two graphs G and \tilde{G} on the same vertex set and let g be a \mathbf{c} -coloring of $V(G)$. The i -homophily of (G, g) and (\tilde{G}, g) could be well the same² but the number of i -isolated vertices can be significantly different. Therefore, knowing that $\omega^i \leq \tilde{\omega}^i$ and $l^i \geq \tilde{l}^i$ would support the claim that (\tilde{G}, g) is more i -homophilous than (G, g) because the relative density of property i is less concentrated in (\tilde{G}, g) than in (G, g) . In conclusion, to assess i -homophily of (G, g) we use the statistics $(Z(\omega^i), Z(l^i))$, where $Z(\omega^i)$ and $Z(l^i)$ are the **z-scores** of ω^i and l^i , respectively. The next theorem, besides summarizing what we have said about the first order moments of the statistics considered so far, also gives the announced expression for $\sigma_{i,j}^2$ and the expression for the variance of L^i . We then exploit these results to compute **z-scores** as a tool for analyzing PPI-networks in the next section.

Theorem 1. *Let G be a graph with n vertices and m edges and let $(\Phi(\mathbf{c}), \mathbb{P}_{n,\mathbf{c}})$ be the probability space of the random \mathbf{c} -colorings, where $\mathbf{c} = (c_1, \dots, c_s)$. Assume $c_i > 0, \forall i \in [s]$. Moreover, let $\pi_3(G)$ denote the number of (not necessarily induced) copies of P_3 in G . For $i, j \in [s]$, consider the random variables $M^{i,j}$ and L^i defined on $(\Phi(\mathbf{c}), \mathbb{P}_{n,\mathbf{c}})$. Then*

²As an example consider the subgraphs G_i and \tilde{G}_i induced by color i in G and \tilde{G} , respectively. If, for some positive integer p , one has $G_i \cong K_p + \overline{K}_{2p}$ and $\tilde{G}_i \cong K_{p-1} + K_{1,p-1} + \overline{K}_p$, then G_i and \tilde{G}_i have the same i -homophily but the number of i -isolated vertices in G_i is twice the number of i -isolated vertices in \tilde{G}_i .

1) for $i \in [s]$ the expected value and the variance of random variable $M^{i,i} = \sum_{uv \in E(G)} Y_{uv}^{i,i}$ where $Y_{uv}^{i,i} = X_u^i X_v^i$ for all $uv \in E(G)$, namely the random number of (i,i) -edges of (G, F) under a random coloring F , are respectively given by

$$\begin{aligned}\overline{m}_{i,i} &= m \frac{c_i^2}{n^2}, \\ \sigma_{i,i}^2 &= m \frac{c_i^2}{n^2} \left(1 - m \frac{c_i^2}{n^2}\right) + 2 \left\{ \left(\frac{c_i^3}{n^3} - \frac{c_i^4}{n^4} \right) \pi_3(G) + \frac{c_i^4}{n^4} \binom{m}{2} \right\};\end{aligned}$$

2) for $i, j \in [s]$, $i \neq j$, the expected value and the variance of random variable $M^{i,j} = \sum_{uv \in E(G)} Y_{uv}^{i,j}$ where $Y_{uv}^{i,j} = (X_u^i X_v^j + X_u^j X_v^i)$ for all $uv \in E(G)$, namely the random number of (i,j) -edges of (G, F) under a random coloring F , are respectively given by

$$\begin{aligned}\overline{m}_{i,j} &= 2m \frac{c_i c_j}{n^2}, \\ \sigma_{i,j}^2 &= 2m \frac{c_i c_j}{n^2} \left(1 - 2m \frac{c_i c_j}{n^2}\right) + 2 \left[\left(\frac{c_i c_j^2 + c_i^2 c_j}{n^3} - 4 \frac{c_i^2 c_j^2}{n^4} \right) \pi_3(G) + 4 \frac{c_i^2 c_j^2}{n^4} \binom{m}{2} \right];\end{aligned}$$

3) for $i \in [s]$ let L^i be the random number of i -isolated vertices of (G, F) under a random coloring F , namely the random variable $L^i = \sum_{v \in E(G)} W_v^i$, where W_v^i is the Bernoulli variable defined as the indicator of the event $(F(v) = i) \wedge (F(w) \neq i, \forall w \in N_G(v))$; then the expected value and the variance of L^i are respectively given by

$$\begin{aligned}\mathbb{E}(L^i) &= \frac{c_i}{n} \sum_{v \in V(G)} \frac{(n - c_i)^{\deg_G(v)}}{(n - 1)^{\deg_G(v)}}, \\ \text{var}(L^i) &= \mathbb{E}(L^i) (1 - \mathbb{E}(L^i)) + \frac{c_i^2}{n^2} \sum_{\substack{(u,v) \in V(G) \\ u \neq v, uv \notin E(G)}} \frac{(n - c_i)^{b(u,v)}}{(n - 2)^{b(u,v)}},\end{aligned}$$

where we have set $b(u,v) = |N_G(u) \cup N_G(v)| = \deg_G(u) + \deg_G(v) - |N_G(u) \cap N_G(v)|$. Clearly, $c_i - L^i$ is the random number of vertices of color i spanned by the (i,i) -edges.

Proof. The expected values $\overline{m}_{i,i}$ and $\overline{m}_{i,j}$, $i \neq j$ have already been computed. Let us prove the formula for the expected value of L^i . By definition W_v^i is the indicator of the event $(F(v) = i) \wedge (F(w) \neq i, \forall w \in N_G(v))$, namely the event that v has color i while all of its neighbors have not. Thus, after (4),

$$\mathbb{E}(W_v^i) = \Pr\{W_v^i = 1\} = \Pr\{X_v^i = 1, D_{N_G(v)}^i = 0\} = \frac{c_i}{n} \Pr\{D_{N_G(v)}^i = 0 \mid X_v^i = 1\} = \frac{c_i}{n} \cdot \frac{(n - c_i)^{\deg_G(v)}}{(n - 1)^{\deg_G(v)}}.$$

Hence, by linearity of expectation

$$\mathbb{E}(L^i) = \frac{c_i}{n} \sum_{v \in V(G)} \frac{(n - c_i)^{\deg_G(v)}}{(n - 1)^{\deg_G(v)}}.$$

Let us compute the variance of the random variables in 1), 2) and 3). Observe that all such variables are sums of Bernoulli random variables, namely they are of the form $S = \sum_{v \in N} B_v$ where N is a finite index

set and B_ν is a Bernoulli random variable for each index $\nu \in N$. The variance of S is thus given by

$$\begin{aligned}
\text{var}(S) &= \mathbb{E}(S^2) - (\mathbb{E}(S))^2 = \mathbb{E}\left(\left(\sum_{\nu \in N} B_\nu\right)^2\right) - (\mathbb{E}(S))^2 = \\
&= \mathbb{E}\left(\sum_{\nu \in N} B_\nu\right) + \mathbb{E}\left(\sum_{\substack{(\nu, \nu') \in N \times N \\ \nu \neq \nu'}} B_\nu B_{\nu'}\right) - (\mathbb{E}(S))^2 = \\
&= \mathbb{E}(S)(1 - \mathbb{E}(S)) + \sum_{\substack{(\nu, \nu') \in N \times N \\ \nu \neq \nu'}} \mathbb{E}(B_\nu B_{\nu'}) = \\
&= \mathbb{E}(S)(1 - \mathbb{E}(S)) + \sum_{\substack{(\nu, \nu') \in N \times N \\ \nu \neq \nu'}} \Pr\{B_\nu = 1 \wedge B_{\nu'} = 1\}
\end{aligned} \tag{6}$$

where we used the fact that $B_\nu = B_\nu^2$ and that $\mathbb{E}(B_\nu B_{\nu'}) = \Pr\{B_\nu = 1 \wedge B_{\nu'} = 1\}$. Let us first specialize the formula above to $M^{i,i}$ and $M^{i,j}$. Notice that in both cases $N = E(G)$ and that the summation set in the last equality of (6) is $E(G) \times E(G) \setminus \{(e, e) \mid e \in E(G)\}$. Denote the latter set by P . Since two edges e and e' of G can have at most one vertex in common, it follows that $P = Q \cup R$ where $Q = \{(e, e') \in P \mid e \sim e'\}$ and $R = \{(e, e') \in P \mid e \not\sim e'\}$ and where we have written $e \sim e'$ if e and e' share a vertex and $e \not\sim e'$ otherwise. Clearly $Q \cap R = \emptyset$. Therefore, if S is either $M^{i,i}$ or $M^{i,j}$, the variance of S is

$$\text{var}(S) = \mathbb{E}(S)(1 - \mathbb{E}(S)) + \sum_Q \Pr\{B_e = 1 \wedge B_{e'} = 1\} + \sum_R \Pr\{B_e = 1 \wedge B_{e'} = 1\}.$$

It is clear that $\Pr\{B_e = 1 \wedge B_{e'} = 1\}$ assumes only two values over the set P : it assumes the value a on Q , and the value b on R . Moreover, since $|P| = (m^2 - m) = 2 \binom{m}{2}$ and since $e \sim e'$ if and only if e and e' spans a P_3 , it follows that

$$|Q| = 2\pi_3(G) = 2 \sum_{v \in V(G)} \binom{\deg_G(v)}{2} \quad \text{and} \quad |R| = 2 \binom{m}{2} - 2\pi_3(G).$$

Therefore, the variance of S assumes the following form

$$\text{var}(S) = \mathbb{E}(S)(1 - \mathbb{E}(S)) + 2 \left[\pi_3(G)(a - b) + \binom{m}{2} b \right]. \tag{7}$$

We obtain expressions for the variance of $M^{i,i}$ and $M^{i,j}$ by plugging the expectation of the corresponding variable in the formula above and specializing a and b for $B_e = Y_e^{i,j}$ and $B_e = Y_e^{i,j}$, with $e = uv$ for some vertices u and v .

Let us start with a , namely, the value of $\Pr\{B_e = 1 \wedge B_{e'} = 1\}$ when $(e, e') \in Q$. Hence $e \sim e'$. After regarding edges as sets of two vertices, one has $e \sim e'$ if and only if $|e \cup e'| = 3$ (recall that the graph is loopless and has no parallel edges). Let $e \cup e' = \{u, v, w\}$ where u is the unique vertex in $e \cap e'$. Recall that for disjoint subsets A and B of $V(G)$ we denote by $\Omega_i(A, B)$ the event that all the vertices of A have color i while all those of B have not. Now, if $S = M^{i,i}$, then $B_e = Y_e^{i,i}$ for all $e \in E(G)$, and thus $a = \Pr\{\Omega_i(\{u, v, w\}, \emptyset)\}$; else, if $S = M^{i,j}$, then $B_e = Y_e^{i,j}$ for all $e \in E(G)$; in this case observe a is the sum of the probability of two mutually exclusive events: the event that u has color i while the vertices in $\{v, w\}$ have color j , namely the event $\Omega_i(\{u\}, \{v, w\}) \wedge \Omega_j(\{v, w\}, \{u\})$, and the the event that u has color j while the vertices in $\{v, w\}$ have color i , namely the event $\Omega_j(\{u\}, \{v, w\}) \wedge \Omega_i(\{v, w\}, \{u\})$. Therefore, by Lemma 1, one has

$$a = \begin{cases} \frac{c_i^3}{n^3} & \text{if } B_e = Y_e^{i,i} \\ \frac{c_i c_j^2 + c_i^2 c_j}{n^3} & \text{if } B_e = Y_e^{i,j} \end{cases}.$$

Let us compute b . In this case $e \cap e' = \emptyset$. Let $e = uv$ and $e' = u'v'$. If $S = M^{i,i}$, then $B_e = Y_e^{i,i}$ for all $e \in E(G)$, and thus a is the probability of the event $\Omega_i(\{u, u', v, v'\}, \emptyset)$, namely the probability that all the four vertices have color i under F ; else, if $S = M^{i,j}$, then $B_e = Y_e^{i,j}$ for all $e \in E(G)$; observe that there are two bipartitions of $\{u, u', v, v'\}$ into sets A and B such that $|A| = |B| = 2$ and neither A nor B induces one of the edges e and e' . Hence b is two times the probability that all the vertices in A have one of the colors i or j and all the vertices in B have the other color. Hence b is four times the probability of the event that all vertices in A have color i and all vertices in B have color j , that is $b = 4\Pr\{\Omega_i(A, B) \wedge \Omega_j(B, A)\}$. Therefore, still by Lemma 1, one has

$$b = \begin{cases} \frac{c_i^4}{n^4} & \text{if } B_e = Y_e^{i,i} \\ 4\frac{c_i^2 c_j^2}{n^4} & \text{if } B_e = Y_e^{i,j} \end{cases}.$$

By plugging the values of a and b (as well as the corresponding expected values) in (7) one achieves the desired expressions for $\sigma_{i,i}^2$ and $\sigma_{i,j}^2$. It only remains to prove the formula for the variance of L^i . By specializing (6) with $S = L^i$, $N = V(G)$, $B_v = W_v^i$ one gets

$$\text{var}(L^i) = \mathbb{E}(L^i)(1 - \mathbb{E}(L^i)) + \sum_{\substack{(u,v) \in V(G) \\ u \neq v}} \Pr\{W_u^i = 1, W_v^i = 1\}$$

and since $\Pr\{W_u^i = 1, W_v^i = 1\} = 0$ whenever u and v are adjacent vertices of G , it follows that

$$\text{var}(L^i) = \mathbb{E}(L^i)(1 - \mathbb{E}(L^i)) + \sum_{\substack{(u,v) \in V(G) \\ u \neq v, uv \notin E(G)}} \Pr\{(X_u^i = 1, X_v^i = 1) \wedge (D_{N_G(u) \cup N_G(v)}^i = 0)\}.$$

Hence, after setting $b(u, v) = |N_G(u) \cup N_G(v)| = \deg_G(u) + \deg_G(v) - |N_G(u) \cap N_G(v)|$, by (11) with $a = 2$ and $b = b(u, v)$ it follows that

$$\Pr\{(X_u^i = 1, X_v^i = 1) \wedge (D_{N_G(u) \cup N_G(v)}^i = 0)\} = \frac{c_i^2}{n^2} \frac{(n - c_i)^{b(u,v)}}{(n - 2)^{b(u,v)}}$$

and after plugging this expression in the latter sum we obtain the stated formula. The proof is thus completed. \square

We are in position to summarize our method.

(8) given the pair (G, g) fix a significance level α . Compute $Z(\omega_i)$ and $Z(\eta_{i,j})$ for each $i, j \in [s]$, $i \neq j$. If $Z(\omega_i) > \frac{1}{\sqrt{\alpha}}$, then declare G i -homophilous at level α . Analogously, if $Z(\eta_{i,j}) > \frac{1}{\sqrt{\alpha}}$, then declare G (i, j) -heterophilous at level α . Notice that, by (5), these are the **z**-scores of the $m_{i,j}$'s (possibly $i = j$). The **z**-score of the number of isolated vertices can be also dealt with in the same way and can be used to refine the analysis.

A couple of facts are worth to be observed.

All of the statistics presented in Theorem 1 have an expression that can be computed in $O(n^3)$ time, n being the order of the input graph. Hence our **z**-score is computationally effective for any input instance. The overall computation time required by the method in (8) is $O(s^2 n^3)$, where s is the number of functional classes.

All of the second order statistics presented in the theorem have an expression that encodes part of the structure of the input graphs, e.g., its number of P_3 's, $2K_2$'s as well as the cardinalities of the set of common neighbors of nonadjacent pair of vertices. This means that the *coefficient of variation* of ω_i , defined as $\sigma_{i,i}/\bar{m}_{i,i}$ is completely determined by G and c_i and that different **c**-colorings (inducing different functional description) have the same scale. In this respect the homophily of the pair (G, g) is an intrinsic measure of the same pair and the coefficient of variation of ω_i is an invariant of the pair (G, \mathbf{c}) . We can thus answer the question “how homophilous the network is?” without resorting to comparisons with other networks.

4. Results

In order to have a first pictorial qualitative perception of homophily in the ten considered PPI networks, we present the values of ratios ω_i and $\eta_{i,j}$ defined in Section 3, in the form of heatmaps. We refer to such ratios as i, j ratios allowing $i = j$ (in this case the ratios are the ω_i ratios). Results are depicted in Figure 1. Color scale is logarithmic, yellow dots on function classes i, j (possibly $i = j$) represent ratios larger than 1 (positive logarithms), while blue dots represent ratios smaller than 1 (negative logarithms). Homophily is clearly readable from all the heatmaps by the yellow dots in all diagonals, showing the density of (i, i) -edges, except for the poorly characterized X function class. Out of some cases (20%), all i, j ratios are smaller than 1, while i, i ratios tend to show very high values.

As a global result, neglecting all i, j pairs where either $i = X$ or $j = X$, we resume that:

- the average value of i, i ratios is 17.8, with standard deviation 22.6, ranging from a 1.12 minimum to a 165.3 maximum;
- 89% of i, i ratios are greater than 3;
- the average value of i, j ratios, with $i \neq j$ is 0.83, with standard deviation 1.43, ranging from a 0.015 minimum to a 25.8 maximum;
- 77.2% of i, j ratios, $i \neq j$, are less than 0.9.

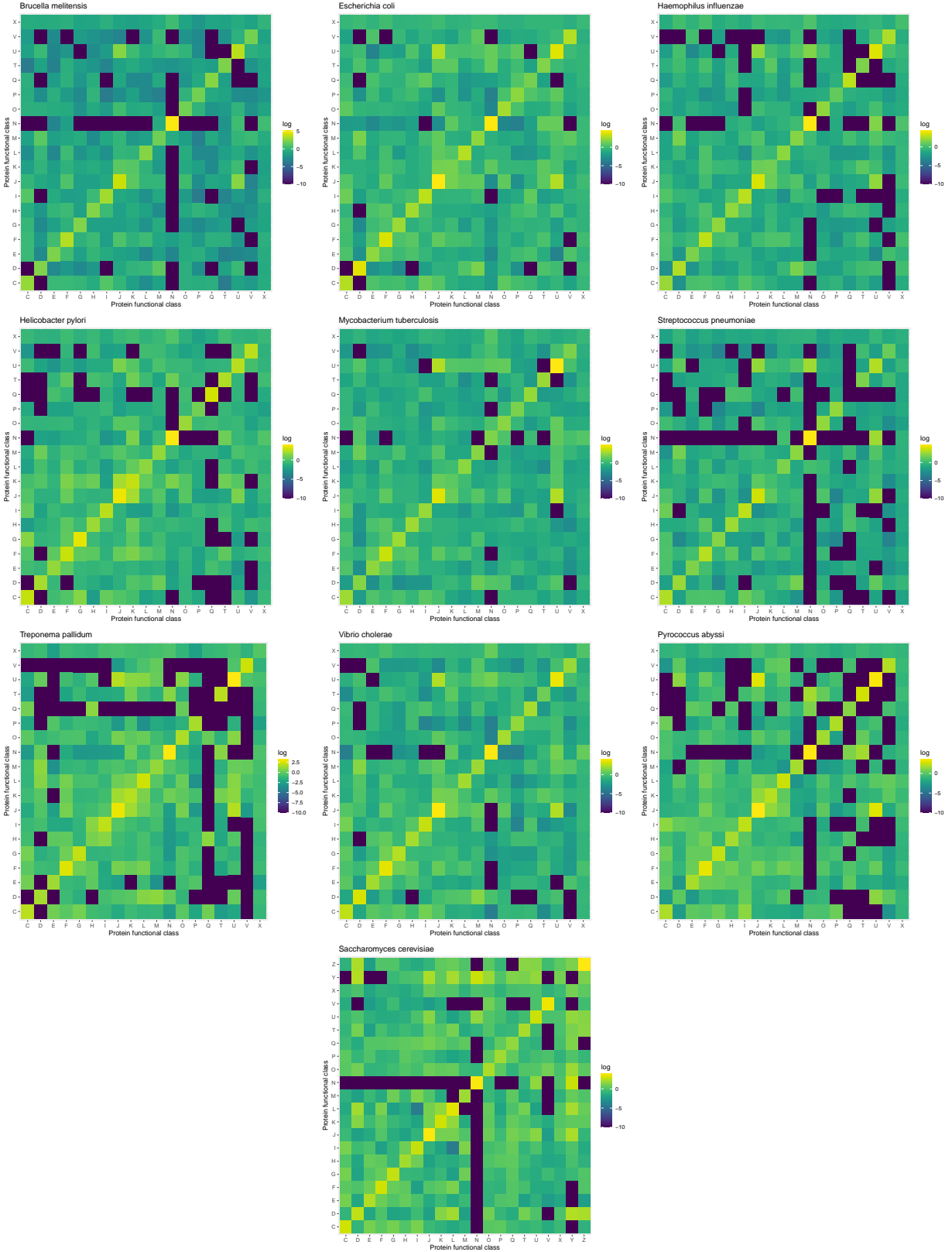


Figure 1: Heatmap plots showing ω_i (along the diagonal) and $\eta_{i,j}$ (for $i \neq j$) ratios for i and j belonging to all considered functional classes, are reported for the ten organism included in the study.

We apply the method described in (8). In details: the density and the number of isolated vertices

were computed for the subgraphs induced by each given protein function class i (as reported in Tab. 2) in the PPI network of each organism o (as reported in Tab. 1. Those statistics were then compared with the expected ones through means and standard deviations, computed as stated in Theorem 1, providing the **z**-score values:

$$Z(\omega_i) = \frac{m_{i,i} - \bar{m}_{i,i}}{\sigma_{i,i}^2}$$

$$Z(L^i) = \frac{L^i - \mathbb{E}(L^i)}{\text{var}(L^i)}$$

For each class and each organism these **z**-scores measure how far the observed values are from the expected ones in terms of standard deviations, or in other words, how many standard deviations the observed values deviate from expected values.

In Fig. 2 and Fig. 3 the **z**-scores related to the density and the number of isolated vertices are reported respectively for each functional class (reported on the x -axis) and each organism (reported with different colors).

A large majority of **z**-scores shows very high values corresponding to extremely significant difference from expected ones. As expected, the exception regards last column related to X class (Function unknown or General function prediction only) showing **z**-score values typically negative including very small values for -14 *Saccharomyces cerevisiae*, -7 *Pyrococcus abyssi* and -6 *Escherichia coli* with only two organisms showing positive values 0.44 *Mycobacterium tuberculosis* and 1.9 *Vibrio cholerae* (2). This typical scenario is consistent with what we could expect from a biological point of view, since it is reasonable that proteins, involved in a common task, could on average preferentially interact or be close to each other in the PPI. Proteins belonging to X class do not share a common task since in most of cases they are not associated to any given functional class, so it is reasonable that they are not likely to interact with each other. Some functional classes seem to show extremely high values, shared among almost all the organisms. It is evident for class J (Translation, ribosomal structure and biogenesis) showing the highest values, reaching huge **z**-scores (335 for *Escherichia coli*, 280 for *Mycobacterium tuberculosis*) always higher than 124. Also class N (Cell motility) shows extremely high **z**-score values reaching 229 for *Brucella mellitensis* and 206 for *Escherichia coli*, with the only exception of *Mycobacterium tuberculosis* - 2.47 - that is anyway more than two standard deviations greater than the expected one. Genes coding for proteins in bacteria are known to typically occur physically close on chromosome, according to the operon paradigm, and it was shown, consistently with our findings (see [15]), that especially genes coding for proteins involved in translation and cell motility task are very close to each other, favoring their synchronous transcription and the interaction of their protein products. In general all classes shows significant values, in particular class F (Nucleotide transport and metabolism), G (Carbohydrate transport and metabolism), H (Coenzyme transport and metabolism), L (Replication, recombination and repair), O (Posttranslational modification, protein turnover, chaperones) and U (Intracellular trafficking, secretion, and vesicular transport) show **z**-score values greater than 10 for all the organisms. Some exceptions concern class D (0.20 for *Pyrococcus abyssi*), K (1.06 for *Streptococcus pneumoniae*), Q (-0.43 for *Streptococcus pneumoniae*, -0.14 for *Treponema pallidum* and 0.87 for *Pyrococcus abyssi*), T (3.33 for *Vibrio cholerae*) and V (4.97 for *Treponema pallidum*).

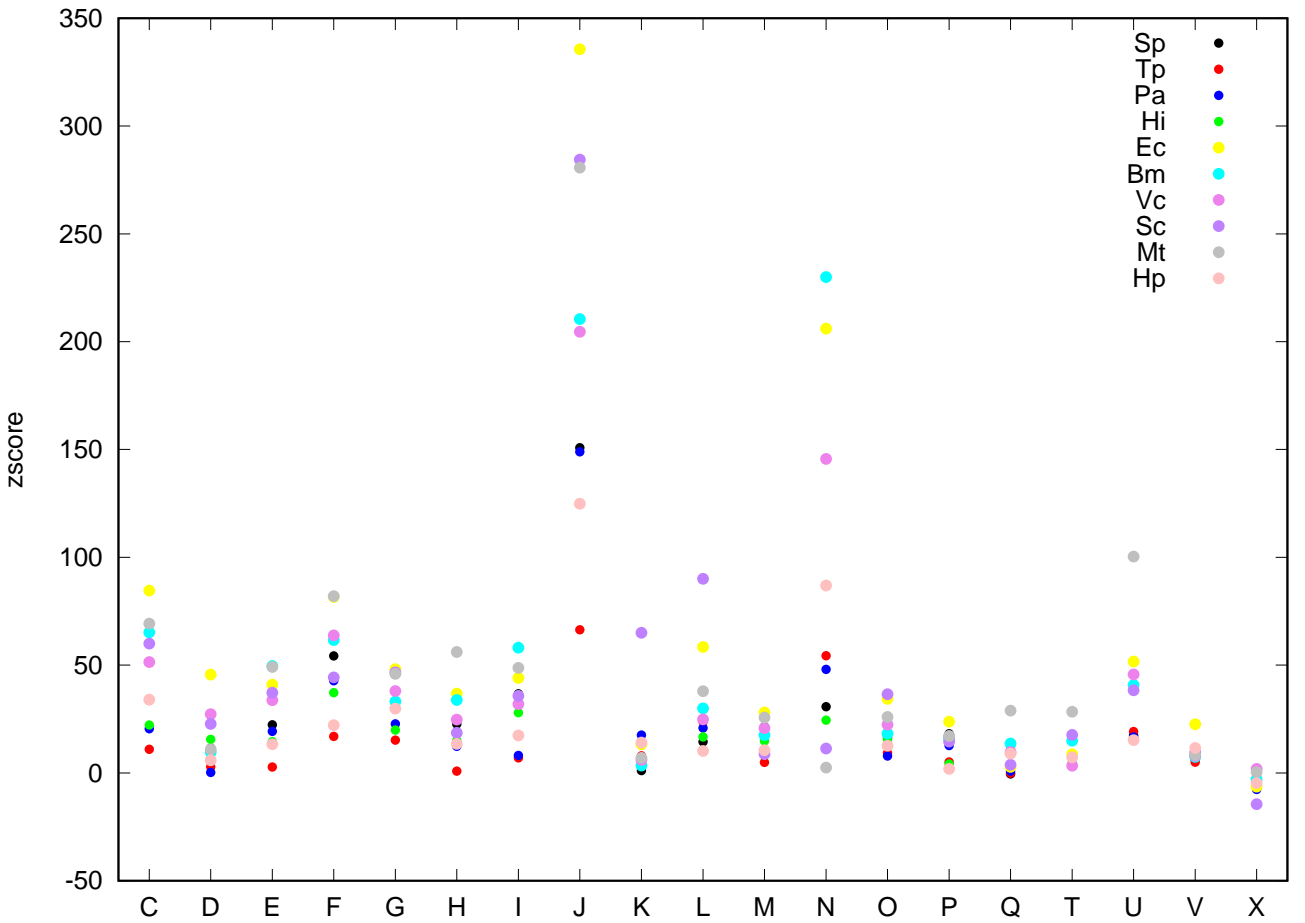


Figure 2: **z**-score density values related to each functional class (x-axis) are reported in different colors (each color representing a different organism as reported in the top right legend of the plot).

Values of **z**-scores related to isolated vertices are typically negative, as expected, consistently with what they biologically represent. A negative **z**-score related to isolated vertices means that subgraphs induced by functional classes contain less isolated vertices than expected. As can be observed in Fig. 3, except for the X class which shows several **z**-score values close to zero and a vast majority of positive values, **z**-scores associated to all other classes assume very low (negative) values (around 75% of values are smaller than -5), that can be considered extremely significant from a statistical point of view. Interestingly, there is an overall reasonable correlation between **z**-scores associated to density and isolated vertices, since the higher the density, the lower the likelihood to find isolated vertices. This correlation was explicitly evaluated and reported in Fig. 4.

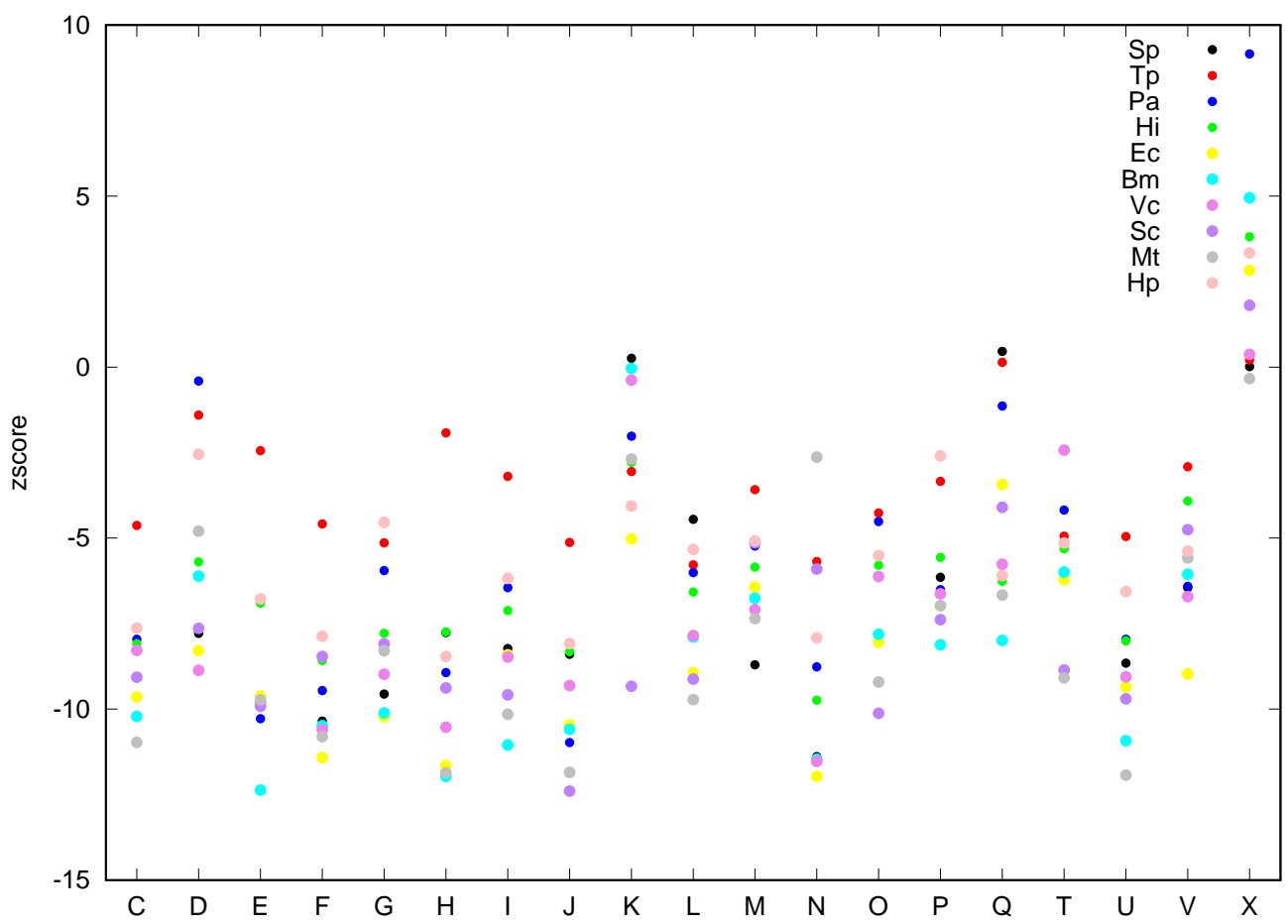


Figure 3: z-score singleton values related to each functional class (x-axis) are reported in different colors (each color representing a different organism as reported in the top right legend of the plot).

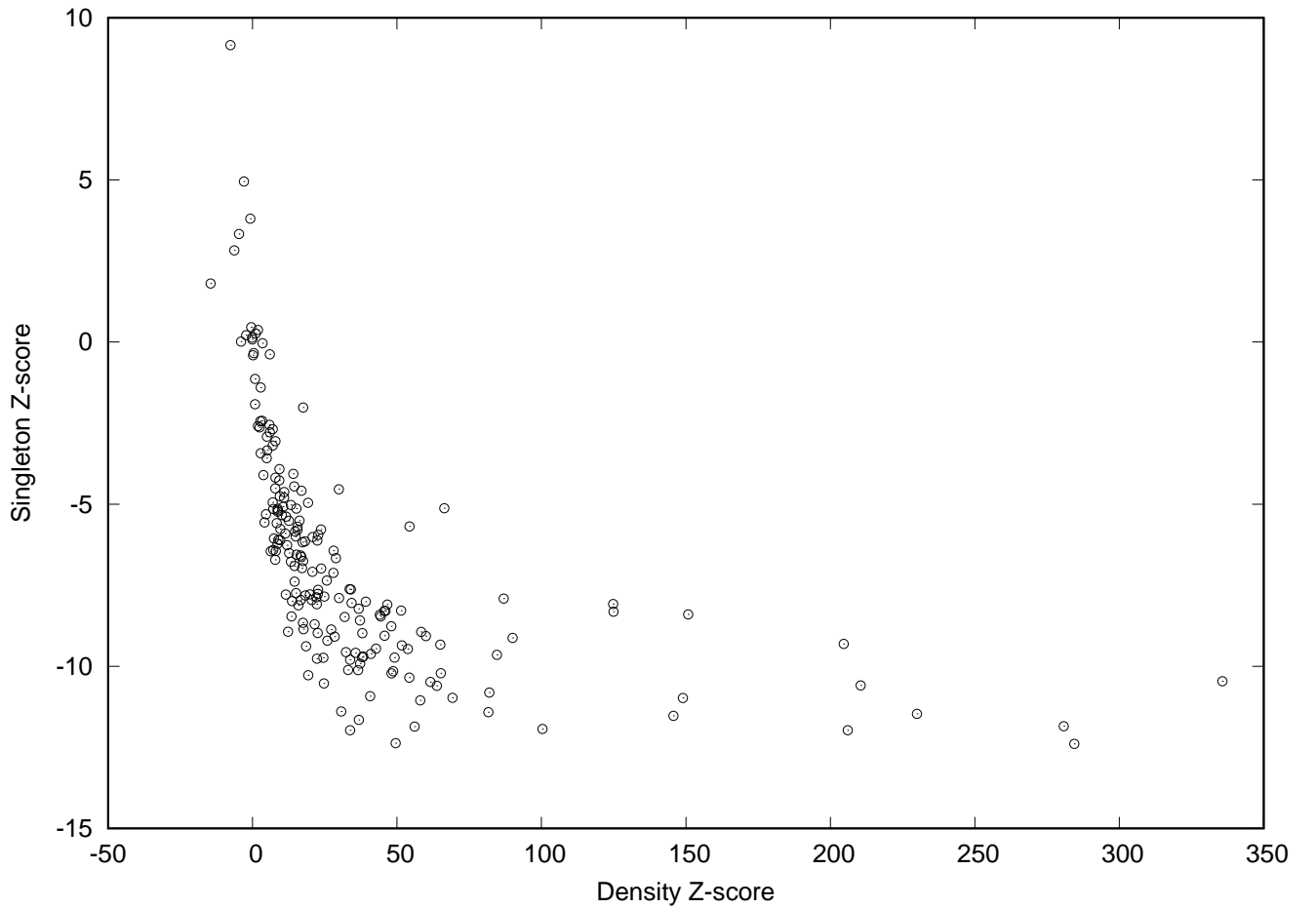


Figure 4: Correlation between **z**-score density values (x-axis) and **z**-score singleton values (y-axis). Each point represents a given functional class of a given organism.

As said in the Section 3.3, Čebyšëv inequality allows us to bound the P-value, associated with the **z**-score of a given statistic, from above simply by squaring the reciprocal of the **z**-score. Such a bound is typically rather loose upper bound on the actual P-value. In this respect our method is rather conservative.

In Fig. 5 P-values obtained in this way are shown. As one can observe a large majority of P-values are under the threshold of 0.05, that is usually considered as reliable with the exceptions already discussed above.

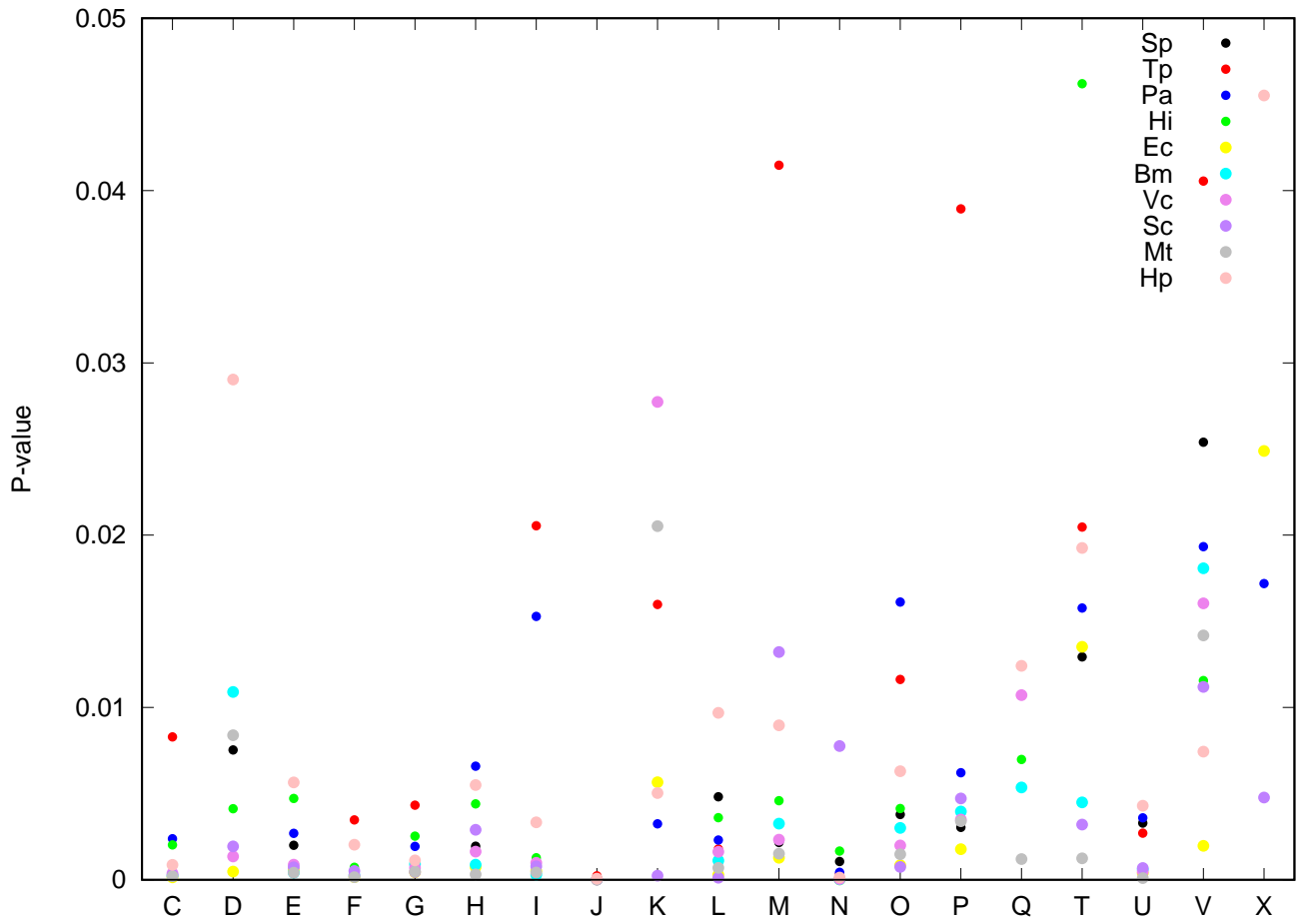


Figure 5: P-values, estimated through Čebyšëv inequality, related to each functional class (x-axis) are reported in different colors (each color representing a different organism as reported in the top right legend of the plot).

z-score density values related to each functional class (x-axis) are reported in different colors (each color representing a different organism as reported in the top right legend).

5. Conclusions and Discussion

In this paper we presented a new approach to assess homophily in networks—especially in PPI networks, which are the focus of this research. The model, summarized in (8), simply computes the **z**-scores of $m_{i,j}$, the number of edges with one end in functional class i and the other end in functional class j (with possibly $i = j$), under the hypothesis that these numbers are samples from the corresponding random variables $M^{i,j}$ under the random coloring model $(\Phi(\mathbf{c}), \mathbb{P}_{n,\mathbf{c}})$ (the null model). These **z**-scores are then compared with $\frac{1}{\sqrt{\alpha}}$, α being the chosen significance level. The idea of random coloring is implicit in [12] from which we also borrowed terminology. As a result, we extended their model to an arbitrary number of colors and made it computationally effective and also quantitative (via the **z**-score). The method is clearly applicable to any kind of network and to any of its functional description. Moreover, we noticed that the coefficients of variations of the $M^{i,j}$'s are invariant for the pair (G, \mathbf{c}) , where G is the network and \mathbf{c} is the profile of the functional description g of G .

Coming to the experimental results, functional protein homophily in PPIs is directly linked to network communities and to the concept of Guilt By Association (GAS). Obtained results provide evidence of the strong homophilic nature of PPIs in terms of protein function, making it reasonable and effective to cluster proteins, according to the topology of the network, in homogeneous groups or communities. As a consequence, our analysis provides strength and reliability to the GAS-oriented paradigm, reinforcing the

concept that proteins, topologically close in the network, are more likely than expected to be involved in similar tasks, or in other words, to share a similar function. In this view, even if it has to be considered an overall and average behavior extrapolated from the whole network, the attempt to infer the function of unknown proteins by analyzing, to some extent, the biological features of neighboring vertices can be considered effective and suitable. It is worth noting that of course the reliability of this process strongly depends on the reliability of edges of PPI networks and a pivotal role can be played by the choice of networks and by the choice of the threshold associated to edges. Ten organism were considered in this study, eighth bacteria, one archea bacterium and one organism belonging to another kingdom (Fungi), *Saccaromyces cerevisiae*. Results shown in Fig. 2, Fig. ?? and Fig. 3 do not highlight significant and evident different behaviors among bacteria and the other two organisms, leading to hypothesize, as expected, that homophily is a typical characteristic of all living organisms.

Acknowledgements

The authors are grateful to Margherita Notarantonio for her contribute in drawing heatmaps.

6. Appendix

In this section, after some preliminaries, we show how to compute probabilities of events related to random **c**-colorings and used throughout the paper.

For a positive integer number a and a nonnegative integer number r , the *r-th falling factorial of a* (also referred to as *r-th falling power of a* in Knuth's terminology [8]) is the number:

$$a^r = \frac{a!}{(a-r)!} = \underbrace{a(a-1)\cdots(a-r+1)}_{r \text{ factors}}$$

and it counts the number of injective mapping from a set of r elements into a set of a elements. One has

- $a^r = 0$ if $r > a$;
- $a^0 = 1$, $a^1 = a$ and $a^a = a!$;
- $a^{r+s} = a^r(a-r)^s$

The reason for Knuth's “falling power” terminology is now clear. Let us come back to the definition of **c**-coloring which we recall here: let V be a set with n elements and, for a positive integer s , let $\mathbf{c} = (c_1, \dots, c_s)$ be a weak composition of n , namely an order sensitive non negative integer vector whose entries add up to n . A **c**-coloring of V is a surjective map $f : V \rightarrow [s]$ such that, for each $i \in [s]$ each *color class* $f^{-1}(i)$ has exactly c_i elements; **c** is the *profile of f*. The *multinomial coefficient with parts* $c_1, c_2 \dots c_s$

$$\binom{n}{\mathbf{c}} = \binom{n}{c_1 c_2 \dots c_s} = \frac{n!}{c_1! c_2! \dots c_s!}$$

counts the **c**-colorings of V . Indeed, the c_1 elements that are mapped to 1 can be chosen in $\binom{n}{c_1}$, the elements that are mapped to 2 can be chosen in $\binom{n-c_1}{c_2}$ among the remaining $n - c_1$. Continuing in this way and taking the product of these binomial coefficients we obtain the expression above. Note that, for $s = 2$, the multinomial coefficient with parts c_1 and c_2 (with $c_2 = n - c_1$), reduces to the binomial coefficient:

$$\binom{n}{c_1 c_2} = \binom{n}{c_1} = \binom{n}{c_2}.$$

Also recall that the binomial coefficient $\binom{n}{r}$ is defined for any pair of positive integers n and r as follows,

$$\binom{n}{r} = \begin{cases} \frac{n!}{r!(n-r)!} & \text{if } 0 \leq r \leq n \\ 0 & \text{otherwise.} \end{cases}$$

Let $J \subseteq [s]$. The *contraction by J* of vector $\mathbf{c} = (c_1, \dots, c_t)$ is the vector \mathbf{c}' obtained from \mathbf{c} by suppressing the entries whose indices are in J . We make use of the following multinomial identity which follows straightforwardly by the definition of the multinomial coefficient:

$$\binom{n}{\mathbf{c}} = \left(\prod_{j \in J} \binom{n}{c_j} \right) \cdot \binom{n - \sum_{j \in J} c_j}{\mathbf{c}'}, \quad (9)$$

where n and \mathbf{c} are as above and \mathbf{c}' is the contraction of \mathbf{c} by J . For instance, if $J = \{1\}$, then $\mathbf{c}' = (c_2, \dots, c_s)$ and the expression above reads as

$$\binom{n}{\mathbf{c}} = \binom{n}{c_1} \cdot \binom{n - c_1}{c_2 \dots c_s}.$$

We now define the notion of random \mathbf{c} -colorings in some more depth. Let $\Phi(\mathbf{c}; V)$ be the set of all \mathbf{c} -colorings of V (in our case $V = V(G)$ for some graph G). When V is understood (as we have assumed throughout the paper) the notation is abridged into $\Phi(\mathbf{c})$. Thus

$$\Phi(\mathbf{c}) = \{f : V \rightarrow [s] \mid f \text{ is surjective}\}.$$

We now equip $\Phi(\mathbf{c})$ with the uniform measure $\mathbb{P}_{n,\mathbf{c}}$

$$\mathbb{P}_{n,\mathbf{c}}(f) = |\Phi(\mathbf{c})|^{-1} = \binom{n}{\mathbf{c}}^{-1}$$

and define the *random \mathbf{c} -coloring of V* , which we denote by F , as the identity map on $\Phi(\mathbf{c})$, namely the random \mathbf{c} -coloring of V is essentially the probability space $(\Phi(\mathbf{c}), \mathbb{P}_{n,\mathbf{c}})$ itself and it can be visualized as the random object F taking the value $f \in \Phi(\mathbf{c})$ with probability $\Pr\{F = f\} = \mathbb{P}_{n,\mathbf{c}}(f)$. A *statistic based on the random \mathbf{c} -coloring F of V* is simply any measurable function on $(\Phi(\mathbf{c}), \mathbb{P}_{n,\mathbf{c}})$, for instance, the indicator X_v^i of the event $(F(v) = i)$, for some $i \in [s]$ and $v \in V$, is one of such. Notice that the inverse image of event $(F(v) = i)$ is the set $\{f \in \Phi(\mathbf{c}) \mid f(v) = i\}$. This is the essence of our statistical model.

For our purposes, for some two disjoint subset A and B of V and some color $i \in [s]$, we are interested in the probability of the event that all the elements of A have color i while all those of B have not. Let $\Omega_i(A, B)$ denote this event. Hence

$$\begin{aligned} \Pr\{\Omega_i(A, B)\} &= \Pr\{(F(a) = i, \forall a \in A) \wedge (F(b) \neq i, \forall b \in B)\} \\ &= \left| \{f \in \Phi_{\mathbf{c}} \mid A \subseteq f^{-1}(i) \subseteq V \setminus B\} \right| / \binom{n}{\mathbf{c}}. \end{aligned}$$

We are also interested in computing the probability of the intersection of two such events for two distinct colors. We summarize these calculations in the next lemma and then we show how to use the lemma for computing the probability of certain simpler events.

Lemma 1. *Let A, A', B, B' be subsets of V and let a, a', b, b' be their respective cardinalities. Suppose $A \cap B = \emptyset$, $A' \cap B' = \emptyset$, $A \cap A' = \emptyset$ and $B \cap B' = \emptyset$ and let $b'' = |B' \cap A|$. Then, for each two distinct colors i and j , one has*

$$\Pr\{\Omega_i(A, B) \wedge \Omega_j(A', B')\} = \left\{ \frac{c_i^a (n - c_i)^b}{n^{a+b}} \right\} \left\{ \frac{c_j^{a'} (n - c_i - c_j)^{b' - b''}}{(n - c_i)^{a' + (b' - b'')}} \right\} \quad (10)$$

Proof. Since the elements of A have to be mapped to i and those of B have not, the elements that have color i can be chosen in $\binom{n-(a+b)}{c_i-a}$ ways. After this choice, we are left with $n - c_i$ elements that have to be assigned to $[s] \setminus \{i\}$ in such a way that all the elements in A' must be mapped to j and those in B' cannot. Among the elements of B' there are possibly some that have been already assigned to i . Therefore we can perform the choice in $\binom{n-c_i-(a'+b'-b'')}{c_j-a'}$ ways. After this choice has been done, we are

left with $n - (c_i + c_j)$ elements that have to be assigned to colors in $[s] \setminus \{i, j\}$, namely with the number of \mathbf{c}' -colorings of a set of $n - (c_i + c_j)$ elements where \mathbf{c}' is the contraction of \mathbf{c} by $\{i, j\}$. It follows that

$$\Pr \{ \Omega_i(A, B) \wedge \Omega_j(A', B') \} = \frac{\binom{n-(a+b)}{c_i-a} \binom{n-c_i-(a'+b'-b'')}{c_j-a'} \binom{n-c_i-c_j}{\mathbf{c}'}}{\binom{n}{c_i} \binom{n-c_i}{c_j} \binom{n-c_i-c_j}{\mathbf{c}'}} ,$$

where we used Formula (9) at the denominator. One obtains Formula (10) after simplifying, expanding the binomial coefficients and resorting to the definition of falling factorial. \square

The way we use the lemma to compute the probability of certain basic events is to read the events as a special case of the event $\Omega_i(A, B) \wedge \Omega_j(A', B')$ and to plug in the formula the corresponding parameters a, b, \dots, b'' . Note that, for any $j \in [s]$, by choosing $A' = B' = \emptyset$ (and $a' = b' = b'' = 0$ correspondingly) makes the event $\Omega_j(A', B')$ almost sure. Hence

$$\begin{aligned} \Pr \{ (F(a) = i, \forall a \in A) \wedge (F(b) \neq i, \forall b \in B) \} &= \Pr \{ \Omega_i(A, B) \} \\ &= \Pr \{ \Omega_i(A, B) \wedge \Omega_j(\emptyset, \emptyset) \} \\ &= \frac{c_i^a (n - c_i)^b}{n^{a+b}} = \frac{c_i^a (n - c_i)^b}{n^a (n - a)^b}. \end{aligned} \quad (11)$$

By, taking $B = \emptyset$ —and hence $b = 0$ —has the effect of suppressing the constraint $(F(b) \neq i, \forall b \in B)$. Therefore, for instance,

$$\Pr \{ F(a) = i, \forall a \in A \} = \Pr \{ \Omega_i(A, \emptyset) \} = \Pr \{ \Omega_i(A, \emptyset) \wedge \Omega_j(\emptyset, \emptyset) \} = \frac{c_i^a}{n^a} \quad (12)$$

and, in particular, for any pair of elements $u, v \in V$ any color $i \in [s]$,

$$\Pr \{ F(u) = i \} = \frac{c_i^1}{n^1} = \frac{c_i}{n} \quad \text{and} \quad \Pr \{ (F(u) = i) \wedge (F(v) = i) \} = \frac{c_i^2}{n^2} = \frac{c_i(c_i - 1)}{n(n - 1)}. \quad (13)$$

Analogously, since for any pair of elements $u, v \in V$ and any two distinct colors $i, j \in [s]$, it holds that

$$(F(u) = i) \wedge (F(v) = j) = \Omega_i(\{u\}, \{v\}) \wedge \Omega_j(\{v\}, \{u\})$$

it follows that two compute the probability of such an event one has to put $a = b = a' = b' = b'' = 1$ in Formula (10) to obtain

$$\Pr \{ (F(u) = i) \wedge (F(v) = j) \} = \frac{c_i^1 c_j^1}{n^2} = \frac{c_i c_j}{n(n - 1)}. \quad (14)$$

References

- [1] Chowdhary R., Zhang J., and Liu JS. 2009. Bayesian inference of protein–protein interactions from biological literature. *Bioinformatics*. 25(12): 1536–1542.
- [2] Deng M, Zhang K, Mehta S, Chen T and Sun F. 2003. Prediction of protein function using protein–protein interaction data. *J Comput Biol*. 10(6): 947–960.
- [3] Easley D. and Kleinberg Jon. 2010. Networks, Crowds, and Markets: Reasoning About a Highly Connected World. Cambridge: Cambridge University Press.
- [4] Gillis J. and Pavlidis P. 2012. “Guilt by Association” Is the Exception Rather Than the Rule in Gene Networks. *PLoS Comput. Biol.* 8(3): e1002444.
- [5] Gulbache N and Lehman S. 2008. The art of community detection. *BioEssays*. 30: 934–938.

- [6] Jansen R., Yu H., Greenbaum D, Kluger Y, Krogan NJ, Chung S, Emili A, Snyder M, Greenblatt JF, Gerstein M. 2003. A Bayesian Networks Approach for Predicting Protein-Protein Interactions from Genomic Data. *Science*. 302(5644): 449-453.
- [7] Jeong H , Mason SP , Barabási AL. and Oltvai ZN. 2001. Lethality and centrality in protein networks. *Nature*. 411: 41-42.
- [8] Knuth D (1997). The Art of Computer Programming, Vol. 1: Fundamental Algorithms Addison-Wesley, Reading, Mass., Third edition.
- [9] Lancichinetti A, Kivelä A, Saramäki J and Fortunato S. 2010. Characterizing the Community Structure of Complex Networks. *PLoS One*. 5(8): e11976.
- [10] Newman M (2006) Modularity and community structure in networks. *Proc Nat Acad Sci USA* 103(23):8577-8582.
- [11] Oliver S. 2000. Guilt-by-association goes global. *Nature*. 403: 601-603.
- [12] Park J. and Barabasi AL. 2007. Distribution of vertex characteristics in complex networks. *Proc Natl Acad Sci USA*. 104(46): 17916 –17920.
- [13] Piovesan D, Giollo M, Ferrari C and Tosa SCE. 2015. Protein function prediction using guilty by association from interaction networks. *Amino Acids*. 47:2583-2592.
- [14] Keshava Prasad TS., et al. 2009. Human protein reference database—2009 update. *Nucleic Acids Res*. 37:D767–D772.
- [15] Santoni D and Romano-Spica V. 2009. Comparative genomic analysis by microbial COGs self-attraction rate. *J Theor Biol*. 258:513-520.
- [16] Szklarczyk D, Morris JH, Cook H, Kuhn M, Wyder S, Simonovic M, Santos A, Doncheva NT, Roth A, Bork P, Jensen LJ, von Mering C. The STRING database in 2017: quality-controlled protein-protein association networks, made broadly accessible. *Nucleic Acids Res*. 45:D362-68.
- [17] Szklarczyk D., Gable AL., Lyon D., Junge A., Wyder S., Huerta-Cepas J., Simonovic M., Doncheva NT., Morris JH., Bork P., Jensen LJ. and von Mering C. 2019. STRING v11: protein-protein association networks with increased coverage, supporting functional discovery in genome-wide experimental datasets. *Nucleic Acids Res*. 47: D607-613.
- [18] von Mering C., Huynen M., Jaeggi D., Schmidt S., Bork P. and Snel B. 2002. STRING: a database of predicted functional associations between proteins. *Nucleic Acids Res*. 31:258-61.
- [19] Von Mering C., Krause R., Snel B., Cornell M., OLiver SG., Fields S. and Bork P. 2002. Comparative assessment of large-scale datasets of protein–protein interactions. *Nature*. 417: 399-403.
- [20] Yang J. and Leskove J. 2015. Defining and evaluating network communities based on ground-truth. *Knowl Inf Syst*. 42:181–213.